physics

MDPI

Article

Log-Normal Superstatistics for Brownian Particles in a Heterogeneous Environment

Maike Antonio Faustino dos Santos [1,*] and Luiz Menon Junior [2]

[1] Department of Physics, Pontifical Catholic University of Rio de Janeiro, Rua Marquês de São Vicente, 225, 22451-900 Rio de Janeiro, Brazil
[2] Department of Physics, Federal University of Paraná, 81531-990 Curitiba, Brazil; menon@fisica.ufpr.br
* Correspondence: santosmaikeaf@gmail.com

Received: 7 September 2020; Accepted: 12 October 2020; Published: 19 October 2020

Abstract: Superstatistical approaches have played a crucial role in the investigations of mixtures of Gaussian processes. Such approaches look to describe non-Gaussian diffusion emergence in single-particle tracking experiments realized in soft and biological matter. Currently, relevant progress in superstatistics of Gaussian diffusion processes has been investigated by applying χ^2-gamma and χ^2-gamma inverse superstatistics to systems of particles in a heterogeneous environment whose diffusivities are randomly distributed; such situations imply Brownian yet non-Gaussian diffusion. In this paper, we present how the log-normal superstatistics of diffusivities modify the density distribution function for two types of mixture of Brownian processes. Firstly, we investigate the time evolution of the ensemble of Brownian particles with random diffusivity through the analytical and simulated points of view. Furthermore, we analyzed approximations of the overall probability distribution for log-normal superstatistics of Brownian motion. Secondly, we propose two models for a mixture of scaled Brownian motion and to analyze the log-normal superstatistics associated with them, which admits an anomalous diffusion process. The results found in this work contribute to advances of non-Gaussian diffusion processes and superstatistical theory.

Keywords: non-Gaussian diffusion; superstatistics; Langevin equation; scaled Brownian motion; random diffusivity

1. Introduction

According to the history of diffusion processes, Brownian motion was reported for the first time in 1828, during experiments with tiny particles contained in pollen grains, immersed in water [1]. This investigation was realized by Robert Brown, and for that reason, it became known as Brownian motion (BM). Nevertheless, only in 1905, after Einstein's research [2,3], was the cause of BM justified by a model that presupposes that there are many collisions of atoms and molecules on a Brownian particle surface. Thereafter, Einstein constructed a diffusion equation, and showed that diffusion of tiny particles (BM) can be characterized by two remarkable features: (i) the probability density function is associated with a Gaussian kernel, as follows

$$G(x,t|D) = \frac{1}{\sqrt{4\pi Dt}} \exp\left[-\frac{x^2}{4Dt}\right], \tag{1}$$

in which D is the diffusion coefficient (diffusivity); and (ii) the mean square displacement (MSD) has a linear growth in time, i.e.,

$$\langle (\Delta x)^2 \rangle = 2Dt, \tag{2}$$

where $\Delta x = x - \langle x \rangle$. Einstein's research paved the way for other models like that; as examples of important names that contributed to distinct formalisms of BM, we can mention: Sutherland [4], Langevin [5] and Smoluchowski [6,7], among others [8]. In subsequent years, sophisticated experiments validated the Brownian models [9]

Prior to the Brownian model's emergence, some experiments revealed that the Brownian diffusion features fail in turbulent flows [10], and charge transport in semiconductors [11], among others [12]. The violation of Brownian features occurs for non-Gaussian shapes of probability density distributions or a nonlinear growth of MSD behavior in time, i.e., $\langle (\Delta x)^2 \rangle \propto t^{\alpha}$ [12,13]. The latter is classified as anomalous diffusion: (i) sub-diffusion for $\alpha < 1$, which is associated with slow diffusion (ii) super-diffusive for $\alpha > 1$, which is associated with a faster diffusion. The anomalous diffusion phenomena are present in complex systems, whose mechanisms are particular to each problem. Among the most useful formalisms to anomalous diffusion are fractional, non-linear, scaled and heterogeneous diffusion processes [14]. Each one includes a vast quantity of tools that are important to approaching anomalous diffusion in different physical scenarios.

Recent experimental insights on single-particle tracking, realized in a variety of animate and inanimate systems, have reported non-Gaussian shapes for distribution, which maintain the MSD growing linearly in time [15]. This new diffusion process is called Brownian yet non-Gaussian diffusion [16,17]. This process was found from the motion of biological macromolecules, proteins and viruses along lipid tubes; and through actin networks [18], swimming Eukaryotic microorganisms [19], diffusion in compartmentalized media [20] and colloidal nanoparticles adsorbed at fluid interfaces [21,22]. Among the main formalisms that admit the approach of Brownian yet non-Gaussian diffusion are superstatistics and subordination [17,23,24]. Furthermore, this formalism assumes a fluctuating diffusivity, though superstatistics can admit fluctuation on different intensive parameters (temperature, viscosity, etc.). In this sense, superstatistics consider an independent probability distribution function (PDF) of a fluctuating parameter that will be used in a new overall PDF which describes the general class of non-Gaussian processes [25].

"Superstatistics" is a term proposed by C. Beck and E.G.D. Cohen in physical contexts that stands for superposition of statistics [26,27]. An analogous idea of the heterogeneous diffusion approach was reported by Kärger [28]. Moreover, other similar mathematical approaches in statistical theories are known as hierarchical or multilevel meddling [29], which is also similar to the Bayesian inference method. In the superstatistics theory framework, there are three main classes of superstatistics [30], which describe a vast quantity of complex systems: χ^2 superstatistics, χ^2-inverse superstatistics and log-normal superstatistics. Each one is fitting for elucidating a different category of physical problems. The first one, χ^2 superstatistics, describes the processes connected to Tsallis statistics [26,31]. The second one, χ^2-inverse superstatistics, has applications in random matrix theory [32,33]. Finally, the third one, log-normal superstatistics, appears associated with turbulent flows [34–36], and in population fluctuations [37] (out of superstatistical context). Particularly, the log-normal superstatistics is associated with a well known log-normal probability distribution function as follows:

$$p(D) = \frac{1}{\sqrt{2\pi}\sigma D} \exp\left[-\frac{(\log[D] - \mu)^2}{2\sigma^2} \right], \tag{3}$$

where σ is the standard deviation, μ is the mean and $\langle D \rangle = e^{\mu + \frac{\sigma^2}{2}}$. Motivated by large amount of research in theoretical and experiment systems with fluctuating diffusivity [20,28,38–43], we investigated the log-normal superstatistics of BM to describe Brownian yet non-Gaussian diffusion, and in the following we consider the log-normal superstatistics associated with scaled Brownian motions to include anomalous diffusion.

This work brings results associated with the superstatistics approach on diffusive systems with fluctuating diffusivity under a new look at log-normal superstatistics. Thereby, it is organized as

follows. In Section 2, we investigate the overall probability for a mixture of Brownian motion and the grey Brownian motion in log-normal superstatistics. We compare the analytical results and simulation results to distribution evolution, including MSD. In the Section 2.1, we consider two approximations of the overall distribution to log-normal superstatistics, and discuss the limitations of each one. In Section 3, we introduce two models for scaled grey Brownian motion and their superstatistics to investigate a mixture of BM in the log-normal superstatistics framework. These models admit diffusion processes that are non-Gaussian and anomalous. Finally, we present the conclusions together with new directions (open problems) associated with the obtained results.

2. From Log-Normal Superstatistics to Brownian Yet Non-Gaussian Diffusion

Let us begin the discussion considering an ensemble of Brownian particles in a complex environment that is constituted by a large amount of patches, each one with a particular diffusivity value [44–46]. This approach changes the diffusivity value for each time-step of the Brownian trajectory; the physical interpretation of this depends on the physical problem. Examples of fluctuating diffusivity systems include the particles walking in a biological environment (such as within cells) in which incorporated distinct places have different diffusivity values that are not evenly dispersed within the cell [47–49]. Another interpretation in the cell environment occurs by considering the fluctuation of particle size due to the fragmentation and agglomeration processes. During these processes, the Brownian particle changes size, and it implies a different reading on the instantaneous diffusivity. Such processes can be associated with superstatistics, which involve Arrhenius' law, the Stokes–Einstein–Flory law or others [50,51]. The fluctuating diffusivity systems (see Figure 1) typically consider a PDF to describe the random choice of D, i.e., $p(D)$, to complete the ensemble average of tracer particles [25]. In this sense, the superstatistics of a mixture of many Brownian diffusion process is defined through an overall PDF as follows [17]:

$$P(x,t) = \int_0^\infty p(D)\frac{1}{\sqrt{4\pi Dt}}\exp\left[-\frac{x^2}{4Dt}\right]dD, \tag{4}$$

where $P(x,t)$ is the probability density function that describes the spatial-temporal behavior of an ensemble of Brownian particles in a heterogeneous environment whose diffusivities are randomly distributed [25], which implies a Non-Gaussian diffusion with linear growth of MSD in time. Equation (4) can be also interpreted as a heterogeneous ensemble of Brownian particles, such that each particle has its own diffusivity [52].

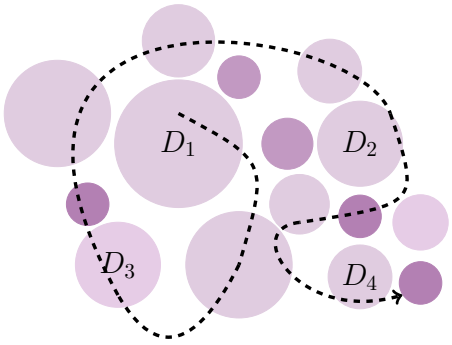

Figure 1. A Brownian particle in a random environment.

The superstatistics of BM ensure that particles explore places within a complex environment with different transport characteristics, such as diffusion coefficient; see reference [53]. Thereby, the overall probability defines the superstatistics of Gaussian statistics corresponding to different diffusivity packets. The above overall probability (Equation (4)) was analyzed in different scenarios in diffusion theory: (i) $p(D)$ as a χ^2 gamma distribution in the context of random diffusivity, to compare

with the diffusive diffusivity model [44], or to describe the movement of many individual small organisms that move with different diffusivities [54]; (ii) $p(N)$ as a χ^2-inverse gamma distribution that depends on particle size to investigate the aggregation and fragmentation process in the context of Laplace diffusion [50]; (iii) $p(D)$ as a stretched exponential to construct a stretched Gaussian diffusion [17,55]; (iv) $p(D)$ Lévy distribution to construct a Lévy process caused by large fluctuations in environment [52]; (v) $p(\beta \propto 1/T)$ as a Mittag–Leffler function to construct generalized Maxwell–Boltzmann distributions [56] and other generalized distributions [57,58], even as truncated-Mittag–Leffler function [59], which was applied in the analysis of the time series of oil price.

In this wide range of scenarios, we consider the probability density function $p(D)$ as a log-normal distribution. An easy feature that we can verify is the linear behavior of MSD in time, i.e., $\langle(\Delta x)^2\rangle = \langle x^2\rangle$ (symmetric distribution around origin), as follows:

$$\begin{aligned} \langle x^2\rangle &= 2t\int_0^\infty Dp(D)dD \\ &= 2D_{\text{eff}} \times t, \end{aligned} \tag{5}$$

where $D_{\text{eff}} = e^{\mu+\frac{\sigma^2}{2}}$ is an effective diffusivity to log-normal superstatistics. The effective diffusivity changes the MSD associated with single Brownian processes (see Equation (2)). Considering $\mu = 0$ and small σ values, we obtain

$$\langle x^2\rangle\Big|_{\sigma\sim 0} \simeq 2t + \sigma^2 t. \tag{6}$$

This is a special approximation that will be discussed in detail in Section 2.1 in the context of a closed-form approximation to the integration defined in Equation (4) in Fourier space.

The equivalent probability distribution in Equation (4) can be computed by generalized grey Brownian motion (ggBM) [60–63], which here we refer to simply as grey Brownian motion, which obeys the following stochastic equation [44]

$$X_t = \sqrt{2D_t} \times W_t, \tag{7}$$

in which $W_t = \int_0^t \xi(t')dt'$ ($\xi(t)$ is white noise) is the Wiener process, and D_t is an independent random variable chosen from a log-normal probability density function. A correspondence between ggBM and overall probability in Equation (4) was proven in Refs. [44,64]. The fluctuating diffusivity is shown in Figure 2 for log-normal distribution with two different σ standard deviation values; the dashed thin line represents the standard diffusivity (constant) associated with Brownian motion. In this context, the trajectory generated for Equation (7) possesses fluctuating diffusivity that "smudges" the white noise, allowing the rise of a grey Brownian trajectory (examples in Figure 3).

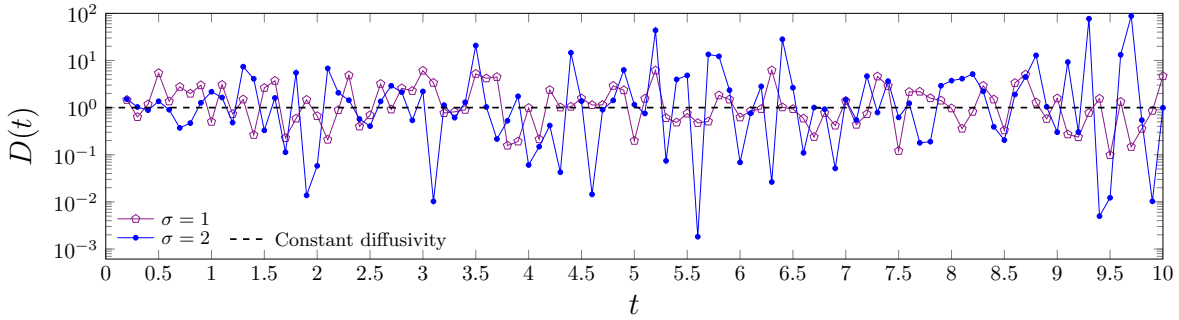

Figure 2. Fluctuating diffusivity of log-normal distribution with $\mu = 0$ and different σ values. The dashed line represents the constant diffusivity case $D = 1$ (implies usual Brownian motion).

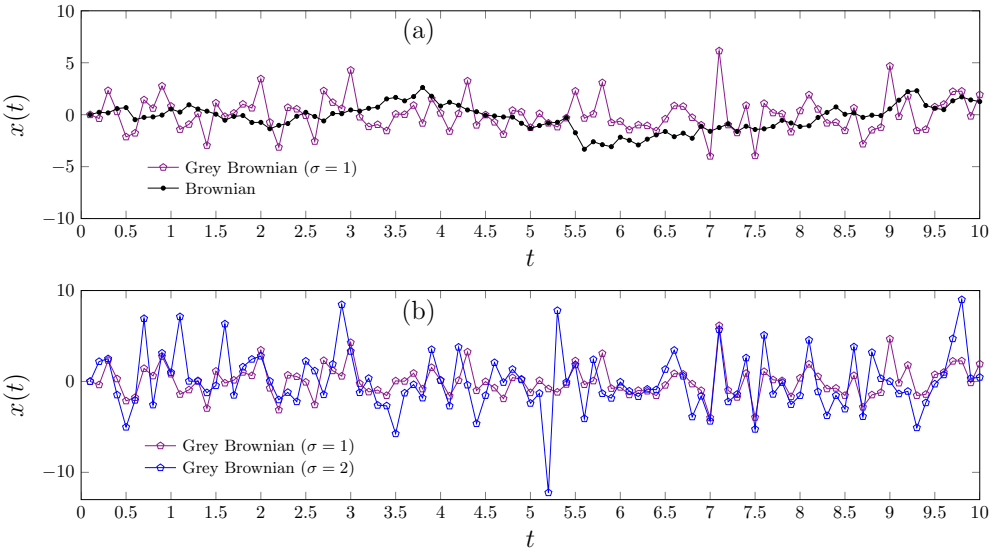

Figure 3. (**a**) The grey Brownian trajectory (D in Equation (7) chosen in log-normal PDF) versus Brownian trajectory ($D = 1$); (**b**) two grey Brownian trajectories (D in Equation (7) for different variance values).

Our next step is analyzing the numerical integration of the log-normal superstatistics average of BM (i.e., Equation (4)), and the correspondence to log-normal grey Brownian motion simulations. To do this, we consider 4×10^6 particles where each one moves according to Equation (7) for simulating the dynamical behavior of grey Brownian motion. In addition, for a short (and a long)time regime we consider steps $dt = 0.01$ ($dt = 1$) with variance and mean of noise equal to one (both). Figure 4 presents the analytical versus simulation results for short and long-time values. We observe that the analytical model (solid curves) agrees perfectly with the simulation data. Figure 5 confirms the previous graphical results for different standard deviation values (case a) and different mean values (case b). Finally, Figure 6 shows the linear time relation of the MSD for two situations, setting one of the parameters (σ, μ) and ranging another. All these graphical results confirm the simulation and analytical agreement. Thereby, the results suggest that the log-normal superstatistics approach of a mixture of Gaussian process implies heavy-tailed distributions, which maintain one of the Brownian features, the linear time relation for MSD.

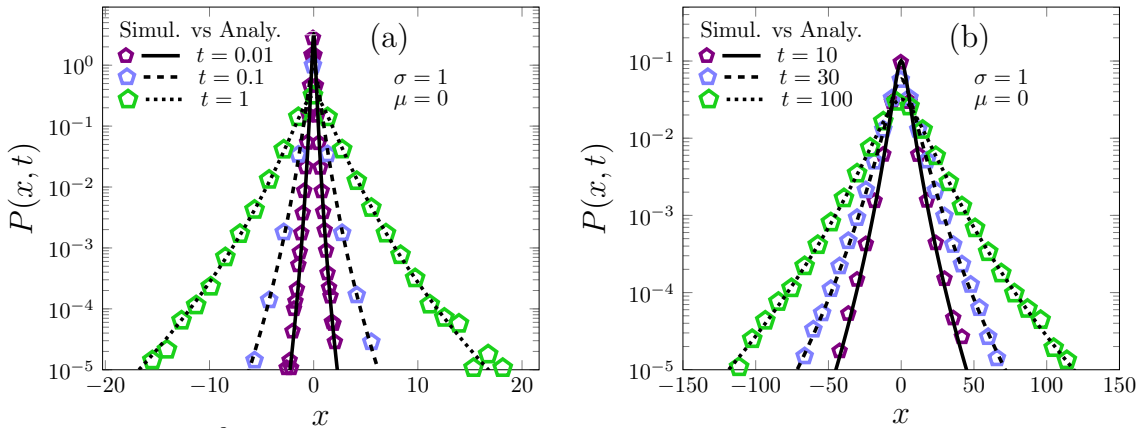

Figure 4. The simulated (pentagon-form symbols) and analytical (solid and dashed) curves to compare the superstatistical average (Equation (4)) with grey Brownian motion where $\sigma = 1$ and $\mu = 0$: (**a**) the PDF evolving for short periods of time; (**b**) the PDF evolving for long periods of time.

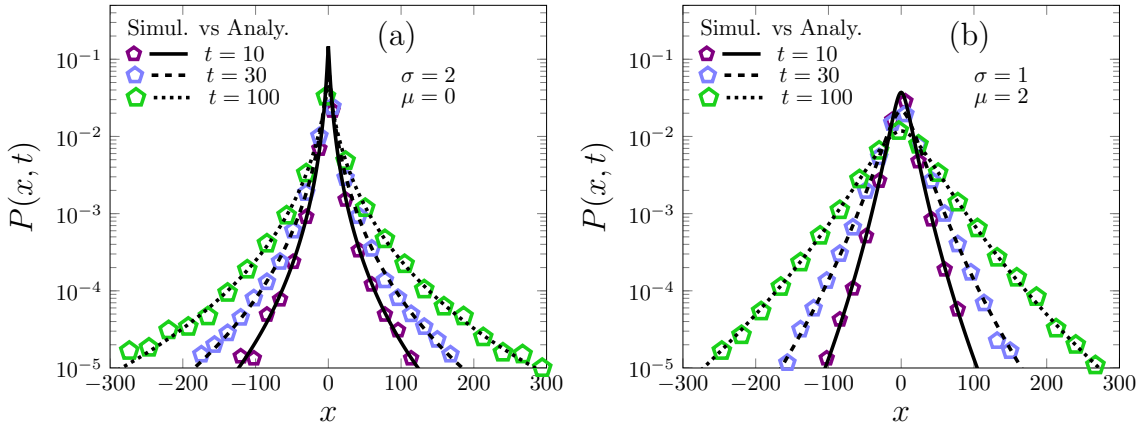

Figure 5. The simulated (pentagon-form symbols) and analytical (solid and dashed) curves for the changes of σ and μ the parameters: (**a**) the PDF with $\sigma = 2$ and $\mu = 0$; (**b**) the PDF with $\sigma = 1$ and $\mu = 2$.

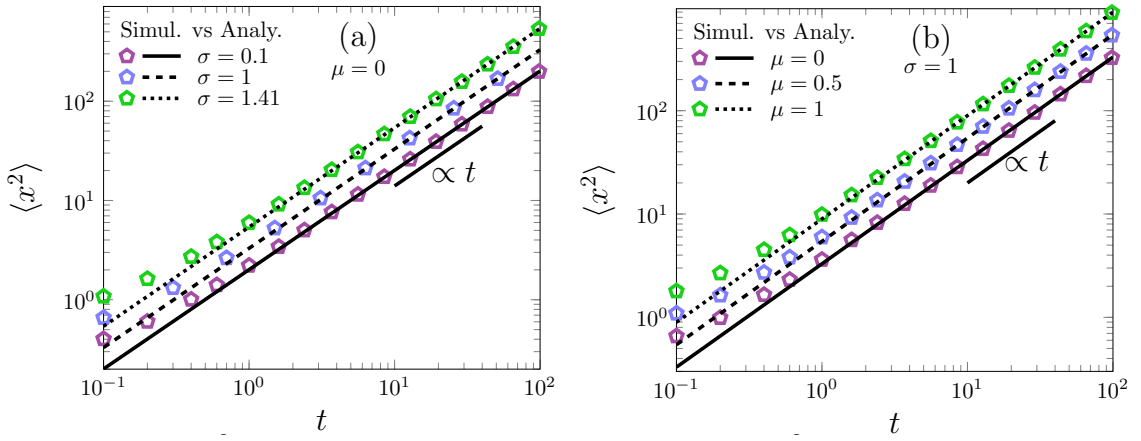

Figure 6. Figures show different MSD behaviors. (**a**) The MSD evolves in time considering $\mu = 0$ and different σ values; (**b**) the MSD evolves in time considering $\sigma = 1$ and different μ values.

2.1. Two Approximations for Log-Normal Superstatistics of Brownian Particles in a Heterogeneous Environment

One of the great challenges in log-normal superstatistics is finding a closed expression for overall density probability. That was not considered until here, because there is not a closed expression for a Laplace transform of log-normal distribution. However, currently, an analysis of closed-form approximation reported by Rojas–Nandayapa [65] for a Laplace transform (leading β to s) of a log-normal PDF has been analyzed through statistical theory. The approximation of the Laplace transform of the log-normal distribution to s is valid for the whole complex domain and $\mu = 0$ is obtained by saddle-point methodology, which implies [66]

$$\begin{aligned} \mathcal{L}\{p(\beta)\} &= \int_0^\infty \frac{1}{\sqrt{2\pi}\sigma\beta} \exp\left[-\frac{(\log[\beta])^2}{2\sigma^2}\right] e^{-s\beta} d\beta \\ &\simeq \frac{1}{\sqrt{1+\mathcal{W}(\sigma^2 s)}} \exp\left[-\frac{1}{2\sigma^2}\left(\mathcal{W}(\sigma^2 s)^2 + 2\mathcal{W}(\sigma^2 s)\right)\right], \end{aligned} \tag{8}$$

where $\mathcal{L}\{p(\beta)\} = \int_0^\infty p(\beta) e^{-s\beta} d\beta$ is the Laplace transform and $\mathcal{W}(z)$ is the Lambert function; this function is the solution of the equation $\mathcal{W}e^{\mathcal{W}} = z$. The Rojas–Nandayapa approximation of the Laplace transform to log-normal PDF for s restricted on the real axis is given by the expression of Equation (8). When restricted to the imaginary axis, it coincides with the approximation of the

characteristic function given by Holgate [67]. Physically, for $\beta = 1/k_{\rm B}T$ (with T and $k_{\rm B}$ being the temperature and Boltzmann constant, respectively) and $s = E$ (energy) we find an approximate closed expression for generalized Boltzmann factor given by Equation (8) in the log-normal superstatistics context, which for large energy values ($E \to \infty$) implies $p(E) \propto (\log[E]))^{-\frac{1}{2}} \exp[-(\log[E])^2]$ in the Rojas–Nandayapa sense [65], which differs from the approximation realized in Holgate's point of view in Refs. [68,69]. Both results are particular cases of Equation (8), when s is a complex number.

Now, within this rich context, we approach two closed approximations for log-normal superstatistics of Brownian particles, one in k-Fourier space and another in x space. The first one applies the Rojas–Nandayapa approximation and Gaussian distribution for Brownian particles in Fourier space. The second one is obtained through the application of the Laplace approximation [70] (or modified Laplace approximation) to approach the overall integration in Equation (4).

To realize the first approximation, we use the Rojas–Nandayapa approximation (8) in the context of mixture of Gaussian processes, considering the Gaussian process in Fourier space as follows:

$$\widetilde{\mathcal{G}}(k,t|D) = \exp[-tDk^2], \tag{9}$$

the Fourier transform is defined by $\mathcal{F}\{f(x)\} = \int_{-\infty}^{\infty} e^{-ixk} f(x)dx$. The integration of overall distribution in Fourier space is written as ensues:

$$\widetilde{P}(k,t) \;=\; \int_0^{\infty} \exp[-Dtk^2] \frac{\exp\left[-\dfrac{(\log[D])^2}{2\sigma^2}\right]}{\sqrt{2\pi}\sigma D} dD. \tag{10}$$

Applying the approximation (8) to Equation (10), one obtains:

$$\widetilde{P}_1(k,t) \;=\; \frac{1}{\sqrt{1+\mathcal{W}(tk^2\sigma^2)}} \exp\left[-\frac{1}{2\sigma^2}\left(\mathcal{W}(tk^2\sigma^2)^2 + 2\mathcal{W}(tk^2\sigma^2)\right)\right], \tag{11}$$

where $\widetilde{P}(k,t) \simeq \widetilde{P}_1$. This closed-form allows us to assume an asymptotic limit for the Lambert function. For $tk^2 \ll 1$ that implies $\mathcal{W}(tk^2\sigma^2) \sim tk^2\sigma^2$, which leads to

$$\begin{aligned} \widetilde{P}_1^{\rm ST}(k,t) \;&\simeq\; \frac{1}{\sqrt{1+tk^2\sigma^2}} \exp\left[-\frac{1}{2\sigma^2}\left((tk^2\sigma^2)^2 + 2tk^2\sigma^2\right)\right] \\ &\simeq\; \exp\left[-tk^2\right], \end{aligned} \tag{12}$$

which implies that a Gaussian diffusion profile is present in a very short times (ST). However, the approximation in Equation (11) is not adequate to determine the analytical behavior of large deviations in space. Furthermore, although this approximation does not perform a perfect match with simulated data, as shown in Figure 7, it provides a suitable background and tools to propose the second approximation over the Gaussian kernel (1) in x space.

To realize the second approximation we have rewritten the overall PDF (4) by use of variable change $y = \log(D)$, which implies

$$P(x,t) \;=\; \int_{-\infty}^{\infty} \frac{\exp\left[-\dfrac{y}{2} - \dfrac{y^2}{2\sigma^2} - e^{-y}\dfrac{x^2}{4t}\right]}{\sqrt{2\pi}\sigma(\sqrt{4\pi t})} dy. \tag{13}$$

Applying the modified Laplace method (see Equations 2.5 and 2.19 of reference [70]), we obtain

$$P_2(x,t) = \frac{\exp\left[-\frac{1}{2\sigma^2}\left(\mathcal{W}\left(e^{\frac{\sigma^2}{2}}\sigma^2\lambda\right)^2 + 2\mathcal{W}\left(e^{\frac{\sigma^2}{2}}\sigma^2\lambda\right)\right) + \frac{\sigma^2}{8}\right]}{\sqrt{4\pi t}\sqrt{1+\mathcal{W}\left(e^{\frac{\sigma^2}{2}}\sigma^2\lambda\right)}}, \tag{14}$$

where $\lambda = x^2/4t$ and $P(x,t) \simeq P_2(x,t)$. For more details about computation of Equation (14), see Appendix A. Figure 7 reveals that approximation two performs better than approximation one. Furthermore, we can analyze two limits that consist of small and large deviations of Equation (14). For small deviations, i.e., $e^{\sigma^2}\sigma^2\lambda \ll 1$ and considering $\mathcal{W}(z) \sim z$, we obtain

$$P_2^{\mathrm{SD}}(x,t) \sim \frac{\exp\left[-\frac{x^2}{4t}e^{\frac{\sigma^2}{2}}\right]}{\sqrt{4\pi t}}. \tag{15}$$

For large deviations, we have $e^{\sigma^2}\sigma^2\lambda \gg 1$ and $\mathcal{W}(z) \sim \log(z)$, which leads to

$$P_2^{\mathrm{LD}}(x,t) \sim \frac{\exp\left[-\frac{(\log(x^2/t))^2}{2\sigma^2}\right]}{\sqrt{4\pi t\log(x^2/t)}}, \tag{16}$$

and represents a distribution with a heavy tail.

The approximations presented are fitting for the simulation data, as shown in Figure 7. Particularly, for short times (small deviations) both approximations present Gaussian behavior. Nevertheless, only the second approximation provides a complete description for large deviations of x value, revealing that log-normal superstatistics in Equation (4) are heavy tailed.

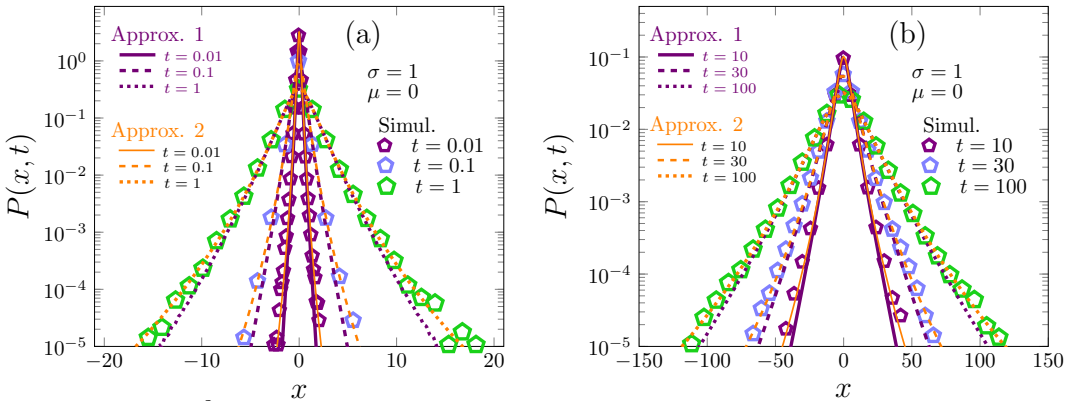

Figure 7. Different probability distributions for simulation data (pentagon-form symbols), the inverse Fourier transform of the first approximation (11) in violet (solid and dashed) curves and the second approximation in Equation (14) in orange (solid and dashed) curves: (**a**) the PDF evolves for short times; (**b**) the PDF evolves for long times.

Now, a new question can be considered: what is a better σ value regime to use in the approximations (11) and (14) in the superstatistics scenario? The answer can be found through MSD behavior, considering that for $\langle x\rangle = 0$ we have $\langle x^2\rangle = -\lim_{k\to 0}\partial_k^2\widetilde{P}(k,t)$ (consider Equation (11)). For the first approximation, the analytical result is $\langle x^2\rangle = 2t + \sigma^2 t$, which coincides with the second moment approximation (see Equation (6)) obtained by assuming small values for standard deviation ($\sigma \ll 1$) on a non-approximated MSD expression (5) with $\mu = 0$. The MSD behavior for second approximation can be calculated by numerical integration. The MSD of both approximations are

confronted with simulation data in Figure 8 for different σ values. This figure shows that for $\sigma < 1$ the first approximation became more suitable to address the log-normal superstatistics of BM. On the other hand, the second approximation is adequate for all σ values simulated.

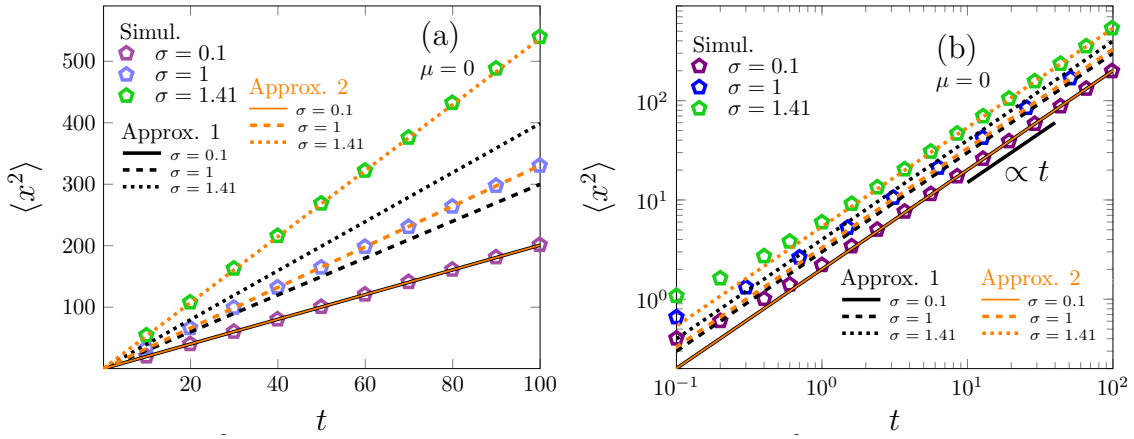

Figure 8. The MSD behavior in time for different σ values shown in (**a**) linear and (**b**) double-log scales. The simulation data are represented by the red, blue and violet curves. Approximation 1 is represented by the black curves, and approximation 2 is represented by the orange curves. For $\sigma = 0.1$ all curves are superposed. Moreover, the second approximation presents a perfect match with the simulation data.

3. Two Models for Scaled Grey Brownian Motion: Log-Normal Superstatistics and Anomalous Diffusion

The scaled Brownian motion (SBM) [71], admits a variable diffusion coefficient in time, i.e., $D(t)$, which is considerable to modeling anomalous diffusion phenomena. Currently, the SBM has been applied in different methods of statistical physics, such as renewal resetting [72], ultra-slow diffusion [73], weak and non-ergodic systems [74,75] and spectral analyses of single trajectory [76]. Here, we consider a stochastic and deterministic diffusion coefficient in time as follows.

$$D(t) = D_t \times f(t), \tag{17}$$

considering D_t is a random variable that describes the fluctuation of the diffusivity and $f(t)$ is a deterministic function in time. We recover the standard situation, i.e., diffusion with time dependence, realizing an average of $D(t)$ on p_D distribution $\langle D(t)\rangle_D = D_{\text{eff}} f(t)$. Thereby, the noise strength in Langevin equation will include a diffusive coefficient with an explicit time dependence that allows us to write two scaled grey BM (sgBM). The first one is

$$X_t^{(1)} = \sqrt{2D_t f(t)} \times W_t, \quad \left(W_t = \int_0^t \xi(t')dt'\right), \tag{18}$$

where the exponent notation $X_t^{(1)}$ refers to the random trajectory of the first model and W_t is the Wiener process. The second model is

$$X_t^{(2)} = \sqrt{2D_t} \times \mathcal{W}_t, \quad \left(\mathcal{W}_t = \int_0^t \sqrt{f(t')}\xi(t')dt'\right), \tag{19}$$

in which the exponent notation $X_t^{(2)}$ refers to the random trajectory and ξ_t is the white noise. Both models of scaled grey Brownian motion (sgBM) for D_t = constant recover the usual ggBM; see Equation (7).

To follow our discussion analysis, see the overall probability distribution for a mixture SBM by way of *Lemma 3.1* stated by Pagnini and Paradisi in Ref. [64] (approached before it was in subordination

laws, see reference [77]). Considering two independent random variables Z_1 and Z_2 whose PDFs are $p_1(Z_1)$ and $p_2(Z_2)$, with $Z_1 \in \mathbb{R}$ and $Z_2 \in \mathbb{R}^+$, let Z be the random variable corresponding to product $Z = Z_1 Z_2^{\gamma}$, and then the PDF $p(z)$ of random variable Z as follows:

$$p(z) = \int_0^{\infty} p_1\left(\frac{z}{\lambda^{\gamma}}\right) p_2(\lambda) \frac{d\lambda}{\lambda^{\gamma}}. \tag{20}$$

A particular family of scaled BM that considers $t_{scaled} = t^{\alpha}$ ($f(t) = \alpha t^{\alpha-1}$) and D = constant, has been applied in experimental and theoretical systems [78–80]. This time-scaled choice implies a second moment that is not linear with time, i.e., $\langle x^2 \rangle \propto t^{\alpha}$, that is especially useful in the anomalous diffusion framework. Therefore, here we consider a family of power-law time scales for both sgBMs (18) and (19) described by

$$X_t^{(1)} = \sqrt{2D_t \alpha t^{\alpha-1}} \times W_t, \tag{21}$$

$$X_t^{(2)} = \sqrt{2D_t} \times \int_0^t \sqrt{\alpha t'^{\alpha-1}} \xi(t') dt', \tag{22}$$

respectively. Keep in mind that D_t is an independent stochastic quantity. To find the overall probability of displacement, we identified Z, Z_1 and Z_2 quantities. According to the Pagnini–Paradisi Lemma represented by Equation (20) with p_1 being a Gaussian process, we have

$$p_{\mathrm{sgBM}}^{(1)}(x,t) = \int_0^{\infty} \mathcal{G}(x, \alpha t^{\alpha}|D) p(D) dD, \tag{23}$$

$$p_{\mathrm{sgBM}}^{(2)}(x,t) = \int_0^{\infty} \mathcal{G}(x, t^{\alpha}|D) p(D) dD, \tag{24}$$

that correspond to models (21) and (22), respectively. Here, the function $\mathcal{G}(x,t|D)$ in the equations above is the standard Gaussian solution (see Equation (1)) and $p(D)$ is the PDF of fluctuating diffusivity. The overall distributions of sgBM's are associated with different scaled diffusion processes, each one connected with $\mathcal{G}(x, \alpha t^{\alpha}|D)$ and $\mathcal{G}(x, t^{\alpha}|D)$, respectively. Thus, both general overall PDs are connected to superstatistics formalism; i.e., $p_{\mathrm{sgBM}} = \int_0^{\infty} p_D \mathcal{G}(x, t^{(i)}|D) dD$ ($i \in \{1,2\}$, 1 for first sgBM model and 2 for the second sgBM model) with $t^{(1)} = tf(t)$ or $t^{(2)} = \int^t f(t) dt$, which may lead to different classes of anomalous diffusion processes. A typical application for superstatistics of scaled Gaussian diffusion processes with exponential diffusivity distribution in the model 2 sense was experimentally investigated to describe the protein/RNA diffusion in cellular environments [47], and protein crowding in lipid bilayers [55]. Additionally, for a detailed discussion about previous considerations of SBM in superstatistics, see reference [81].

Now, we will confront the superstatistical approach with simulations of sgBM models. Thereby, we consider the simulation (SM) process with 10^6 trials (particles number) with $dt = 1$ in Langevin Equation (18) with fluctuating diffusivity following the log-normal distribution (3). Figure 9a,b compares the distributions (23) and (24) (analytic approach) to simulations of sgBM models ($dt = 1$ in SM) for $t = 30$ and different $\alpha = 2$ and $\alpha = 0.5$, respectively. The Figure 10a,b shows how the second moment ($dt = 0.01$ in SM) evolves in time for different $\alpha = 2$ and $\alpha = 0.5$, respectively. In the MSD analysis, we clearly perceive that the anomalous diffusion emergence occurs with a difference between them, yet this difference is more drastic than a multiplicative constant for $f(t)$ functions that are not power-law functions. The generalized second moment are $\langle x^2 \rangle \simeq 2tf(t)$ for sgBM model 1, and $\langle x^2 \rangle \simeq 2\int^t f(t')dt'$ for sgBM model 2.

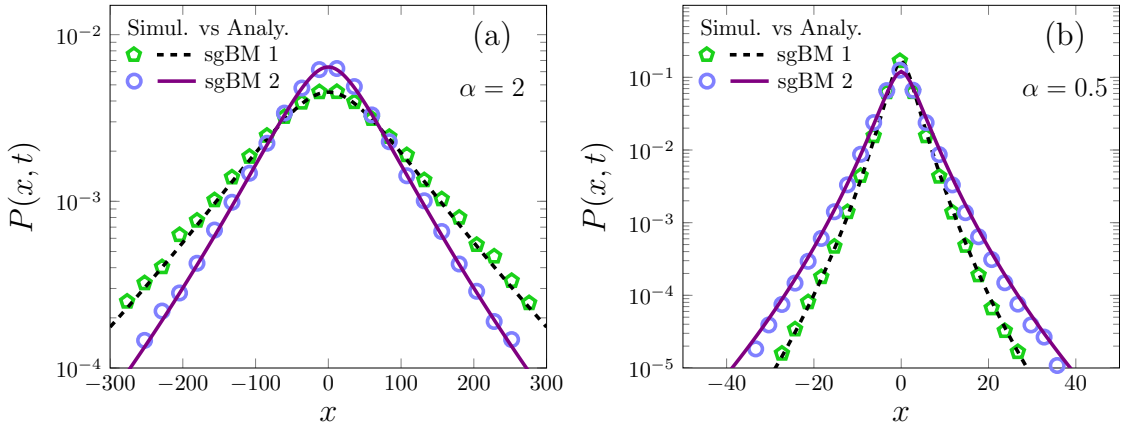

Figure 9. The PDFs associated with two models of scaled grey Brownian motion (sgBM) for $t = 30$, with fluctuating diffusivity following the log-normal distribution (3). Specifically, the PDF profiles for analytical 1 (23) and analytical 2 (24) compared with simulation sgBM 1 (18) and simulation sgBM 2 (19), respectively, are shown. The comparisons are shown for (**a**) $\alpha = 2$ and (**b**) $\alpha = 0.5$.

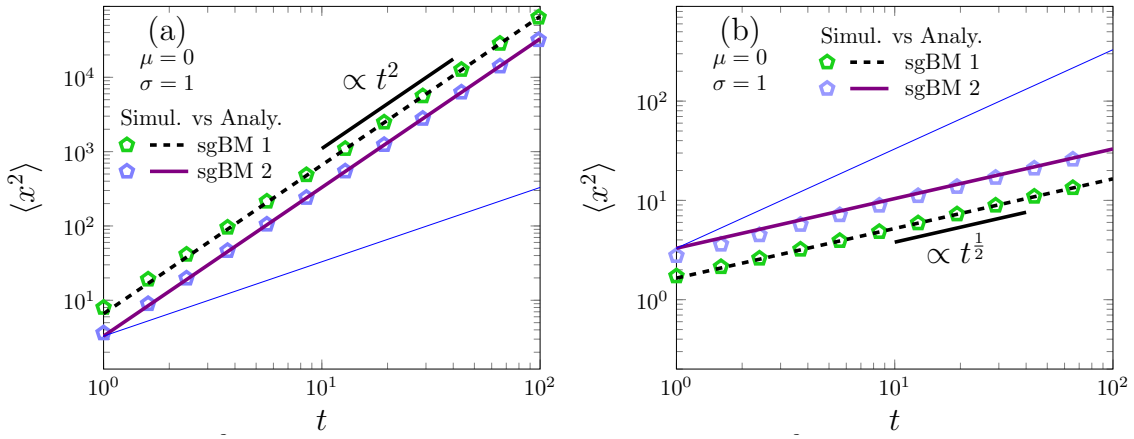

Figure 10. The MSD behaviors associated with two models of scaled grey Brownian motion (sgBM) with fluctuating diffusivity following the log-normal distribution (3). Specifically, the MSD profiles are shown for analytical 1 (23) (analytical 2 (24)) compared with simulation sgBM 1 (18) (simulation sgBM 2 (19)). The comparisons are shown for (**a**) $\alpha = 2$ and (**b**) $\alpha = 0.5$. The thin blue line in both figures represents the standard grey Brownian motion, i.e., $\langle x^2 \rangle = 2D_{\text{eff}}t$ for $\alpha = 1$.

4. Conclusions

In this work, we investigated the influence of log-normal superstatistics on the ensemble of Brownian particles in a complex environment whose diffusivities are randomly distributed in space. We have shown that log-normal superstatistics of Gaussian processes can be obtained from numerical integration of overall probability and that implies Brownian yet non-Gaussian diffusion associated with heavy-tailed distributions. This way, we showed that this result agrees with the generalized grey Brownian motion process. Subsequently, we analyzed two closed-form approximations, each one proper to the application of the log-normal superstatistics over BM in Fourier space and x-coordinate space, respectively. The first approximation agrees with simulation results only for small values of standard variation, i.e., $\sigma < 1$ and $\mu = 0$. The second approximation agrees with simulation results for σ values considered.

Further, another relevant approach investigated in this work was to consider the grey generalized Brownian motion in the context of scaled BM. To do this, we introduced two models of scaled grey Brownian motion (sgBM) and their respective overall distributions. Then, we presented a series

of diffusive analysis within log-normal superstatistical context through analytical and simulation results, thereby showing that both sgBM models imply rich classes of non-Gaussian diffusion with anomalous diffusion.

Our research contributed to this broader scenario of non-Gaussian diffusion processes and superstatistics. Furthermore, this research opens the ways for investigation of new insights associated with the results (open problems); some of them include:

- The construction and analysis of a PDF $p_D(t)$ for diffusive diffusivity dynamics [82] that for long times converges to log-normal distribution. Additionally, the analysis of the problem in the context of a non-equilibrium ggBM model [44].
- The analysis of the closed approximation (8) for log-normal superstatistics into extreme values theory [69].
- The investigation of the sgBM models for different time-scale ($f(t)$ functions [73]).
- The analyses of the Langevin equation with fractional noise [83,84] and log-normal superstatistics for random diffusivity.

Author Contributions: Conceptualization, M.A.F.d.S. and L.M.J.; methodology, M.A.F.d.S. and L.M.J.; validation, M.A.F.d.S. and L.M.J.; formal analysis, M.A.F.d.S.; investigation, M.A.F.d.S. and L.M.J.; data curation, M.A.F.d.S. and L.M.J.; writing–original draft preparation, M.A.F.d.S.; writing–review and editing, M.A.F.d.S.; All authors have read and agreed to the published version of the manuscript.

Funding: This research received no external funding.

Acknowledgments: We acknowledge financial support by the Coordenação de Aperfeiçoamento de Pessoal de Nível Superior—Brazil (CAPES). We thank the referees for their comments and recommendations.

Conflicts of Interest: The authors declare no conflict of interest.

Appendix A

The second approximation made in Equation (14) can be performed through the modified Laplace method introduced by Butler (see Equations *2.5* and *2.19* of reference [70]) defined by

$$\int_a^b \exp\left[-h(y)\right] dy \simeq \sqrt{\frac{2\pi}{h''(y_m)}} \exp\left[-h(y_m)\right], \tag{A1}$$

where $h(y) > 0$ and y_m is the minimum point of $h(y)$ over (a, b).

Firstly, assuming the variable change $y = \log(D)$ in Equation (4) (begin $p(D)$ defined by Equation (3)), we rewrite it as follows:

$$P(x,t) = \int_{-\infty}^{\infty} \frac{\exp\left[-\frac{y}{2} - \frac{y^2}{2\sigma^2} - e^{-y}\frac{x^2}{4t}\right]}{\sqrt{2\pi}\sigma\sqrt{4\pi t}} dy. \tag{A2}$$

Hence, for approximation (A1) we have that $P(x,t) \simeq P_2(x,t)$, $P_2(x,t)$ being defined by

$$P_2(x,t) = \sqrt{\frac{2\pi}{h''(y_m)}} \frac{\exp\left[-h(y_m)\right]}{\sqrt{2\pi}\sigma\sqrt{4\pi t}}, \tag{A3}$$

where $h(y) = \frac{y}{2} - \frac{y^2}{2\sigma^2} - e^{-y}\frac{x^2}{4t}$ and y_m is the minimal point. Thereby, we obtain

$$h = \frac{y}{2} + \frac{y^2}{2\sigma^2} + e^{-y}\lambda, \tag{A4}$$

$$h' = \frac{1}{2} + \frac{y}{\sigma^2} - e^{-y}\lambda, \tag{A5}$$

$$h'' = \frac{1}{\sigma^2} + e^{-y}\lambda, \tag{A6}$$

in which $\lambda = x^2/4t$. For $h^{(1)} = 0$ implies $(\frac{\sigma^2}{2} + y)e^y = \lambda\sigma^2$, yielding

$$y_m = \mathcal{W}\left(e^{\frac{\sigma^2}{2}}\sigma^2\lambda\right) - \frac{\sigma^2}{2}, \tag{A7}$$

which is the minimum point and $\mathcal{W}(z)$ is the Lambert function. Thereby, rewriting the approximation (A3) in terms of λ, obtains

$$P_2(x,t) = \frac{(\sigma\sqrt{4\pi t})^{-1}}{\sqrt{h''_\lambda}} \exp\left[-\overbrace{\left(\frac{\mathcal{W}_\lambda}{2} - \frac{\sigma^2}{4}\right)}^{y/2} - \frac{1}{2\sigma^2}\overbrace{\left(\mathcal{W}_\lambda^2 - \sigma^2\mathcal{W}_\lambda + \frac{\sigma^4}{4}\right)}^{y^2} - \overbrace{\left(\frac{\mathcal{W}_\lambda}{\sigma^2}\right)}^{e^{-y}\lambda}\right], \tag{A8}$$

where $\mathcal{W}_\lambda = \mathcal{W}\left(e^{\frac{\sigma^2}{2}}\sigma^2\lambda\right)$. That implies

$$P_2(x,t) = \frac{\exp\left[-\frac{1}{2\sigma^2}\left(\mathcal{W}\left(e^{\frac{\sigma^2}{2}}\sigma^2\lambda\right)^2 + 2\mathcal{W}\left(e^{\frac{\sigma^2}{2}}\sigma^2\lambda\right)\right) + \frac{\sigma^2}{8}\right]}{\sqrt{4\pi t}\sqrt{1 + \mathcal{W}\left(e^{\frac{\sigma^2}{2}}\sigma^2\lambda\right)}}, \tag{A9}$$

This defines the second approximation considered in Section 2.1. As in the first approximation of Rojas et al. [66], our approximation through the modified Laplace transform method is not restricted to large λ values.

References

1. Brown, R. Mikroskopische Beobachtungen über die im Pollen der Pflanzen enthaltenen Partikeln, und über das allgemeine Vorkommen activer Molecüle in organischen und unorganischen Körpern. *Ann. Der Phys.* **1828**, *90*, 294–313. [CrossRef]
2. Einstein, A. On the theory of the Brownian movement. *Ann. Phys.* **1906**, *19*, 371–381. [CrossRef]
3. Einstein, A. *Investigations on the Theory of the Brownian Movement*; MACourier Corporation: Chelmsford, UK, 1956.
4. Sutherland, W. LXXV. A dynamical theory of diffusion for non-electrolytes and the molecular mass of albumin. *Lond. Edinburgh Dublin Philos. Mag. J. Sci.* **1905**, *9*, 781–785. [CrossRef]
5. Langevin, P. Sur la théorie du mouvement brownien. *Compt. Rendus* **1908**, *146*, 530–533.
6. Smoluchowski, M.v. Zur kinetischen Theorie der Brownschen Molekular Bewegung und der Suspensionen. *Ann. Phys.* **1906**, *21*, 756–780. [CrossRef]
7. Smoluchowski, M.V. Über Brownsche Molekularbewegung unter Einwirkung äußerer Kräfte und deren Zusammenhang mit der verallgemeinerten Diffusionsgleichung. *Ann. Phys.* **1916**, *353*, 1103–1112. [CrossRef]
8. Risken, H. Fokker-Planck Equation. In *The Fokker-Planck Equation*; Springer: Berlin/Heidelberg, Germany, 1996; pp. 63–95.
9. Hänggi, P.; Marchesoni, F. Introduction: 100 years of Brownian motion. *Chaos* **2005**, *15*, 26101. [CrossRef]
10. Richardson, L.F. Atmospheric diffusion shown on a distance-neighbour graph. *Proc. R. Soc. Lond. Ser. A: Math. Phys. Eng. Sci.* **1926**, *110*, 709–737. [CrossRef]
11. Scher, H.; Montroll, E.W. Anomalous transit-time dispersion in amorphous solids. *Phys. Rev. B* **1975**, *12*, 2455. [CrossRef]
12. Metzler, R.; Klafter, J. The random walk's guide to anomalous diffusion: a fractional dynamics approach. *Phys. Rep.* **2000**, *339*, 1–77. [CrossRef]
13. dos Santos, M. A. F. Analytic approaches of the anomalous diffusion: A review. *Chaos Solitons Fractals* **2019**, *124*, 86–96. [CrossRef]

14. Metzler, R.; Jeon, J.H.; Cherstvy, A.G.; Barkai, E. Anomalous diffusion models and their properties: Non-stationarity, non-ergodicity, and ageing at the centenary of single particle tracking. *Phys. Chem. Chem. Phys.* **2014**, *16*, 24128–24164. [CrossRef]
15. Metzler, R. Gaussianity Fair: The Riddle of Anomalous yet Non-Gaussian Diffusion. *Biophys. J.* **2017**, *112*, 413–415. [CrossRef] [PubMed]
16. Wang, B.; Kuo, J.; Bae, S.C.; Granick, S. When Brownian diffusion is not Gaussian. *Nat. Mater.* **2012**, *11*, 481–485. [CrossRef] [PubMed]
17. Chechkin, A.V.; Seno, F.; Metzler, R.; Sokolov, I.M. Brownian yet non-Gaussian diffusion: from superstatistics to subordination of diffusing diffusivities. *Phys. Rev. X* **2017**, *7*, 021002. [CrossRef]
18. Wang, B.; Anthony, S.M.; Bae, S.C.; Granick, S. Anomalous yet brownian. *Proc. Natl. Acad. Sci. USA* **2009**, *106*, 15160–15164. [CrossRef]
19. Leptos, K.C.; Guasto, J.S.; Gollub, J.P.; Pesci, A.I.; Goldstein, R.E. Dynamics of enhanced tracer diffusion in suspensions of swimming eukaryotic microorganisms. *Phys. Rev. Lett.* **2009**, *103*, 198103. [CrossRef]
20. Ślęzak, J.; Burov, S. From diffusion in compartmentalized media to non-Gaussian random walks. *arXiv* **2019**, arXiv:1909.11395.
21. Dutta, S.; Chakrabarti, J. Anomalous dynamical responses in a driven system. *Europhys. Lett.* **2016**, *116*, 38001. [CrossRef]
22. Wang, D.; Hu, R.; Skaug, M.J.; Schwartz, D.K. Temporally anticorrelated motion of nanoparticles at a liquid interface. *J. Phys. Chem. Lett.* **2015**, *6*, 54–59. [CrossRef]
23. Lanoiselée, Y.; Grebenkov, D.S. Non-Gaussian diffusion of mixed origins. *J. Phys. Math. Theor.* **2019**, *52*, 304001. [CrossRef]
24. Barkai, E.; Burov, S. Packets of Diffusing Particles Exhibit Universal Exponential Tails. *Phys. Rev. Lett.* **2020**, *124*, 060603. [CrossRef]
25. Metzler, R. Superstatistics and non-Gaussian diffusion. *Eur. Phys. J. Spec. Top.* **2020**, *229*, 711–728. [CrossRef]
26. Beck, C. Dynamical foundations of nonextensive statistical mechanics. *Phys. Rev. Lett.* **2001**, *87*, 180601. [CrossRef]
27. Beck, C.; Cohen, E.G. Superstatistics. *Physica A* **2003**, *322*, 267–275. [CrossRef]
28. Kärger, J. NMR self-diffusion studies in heterogeneous systems. *Adv. Colloid Interface Sci.* **1985**, *23*, 129–148. [CrossRef]
29. Goldstein, H. *Multilevel Statistical Models*; John Wiley & Sons: Hoboken, NJ, USA, 2011; Volume 922.
30. Beck, C.; Cohen, E.G.; Swinney, H.L. From time series to superstatistics. *Phys. Rev. E* **2005**, *72*, 056133. [CrossRef] [PubMed]
31. Tsallis, C. Possible generalization of Boltzmann-Gibbs statistics. *J. Stat. Phys.* **1988**, *52*, 479–487. [CrossRef]
32. Abul-Magd, A. Superstatistics in random matrix theory. *Physica A* **2006**, *361*, 41–54. [CrossRef]
33. Abul-Magd, A.; Dietz, B.; Friedrich, T.; Richter, A. Spectral fluctuations of billiards with mixed dynamics: from time series to superstatistics. *Phys. Rev. E* **2008**, *77*, 046202. [CrossRef]
34. Beck, C. Superstatistics in hydrodynamic turbulence. *Phys. D Nonlinear Phenom.* **2004**, *193*, 195–207. [CrossRef]
35. Beck, C. Lagrangian acceleration statistics in turbulent flows. *Europhys. Lett.* **2003**, *64*, 151. [CrossRef]
36. Abe, S. Fluctuations of entropy and log-normal superstatistics. *Phys. Rev. E* **2010**, *82*, 011131. [CrossRef] [PubMed]
37. Allen, A.P.; Li, B.L.; Charnov, E.L. Population fluctuations, power laws and mixtures of lognormal distributions. *Ecol. Lett.* **2001**, *4*, 1–3. [CrossRef]
38. Yamamoto, E.; Akimoto, T.; Mitsutake, A.; Metzler, R. Universal relation between instantaneous diffusivity and radius of gyration of proteins in aqueous solution. *arXiv* **2020**, arXiv:2009.06829.
39. Miyaguchi, T.; Akimoto, T.; Yamamoto, E. Langevin equation with fluctuating diffusivity: A two-state model. *Phys. Rev. E* **2016**, *94*, 012109. [CrossRef] [PubMed]
40. Uneyama, T.; Miyaguchi, T.; Akimoto, T. Relaxation functions of the Ornstein-Uhlenbeck process with fluctuating diffusivity. *Phys. Rev. E* **2019**, *99*, 032127. [CrossRef]
41. Manzo, C.; Torreno-Pina, J.A.; Massignan, P.; Lapeyre, G.J., Jr.; Lewenstein, M.; Parajo, M.F.G. Weak ergodicity breaking of receptor motion in living cells stemming from random diffusivity. *Phys. Rev. X* **2015**, *5*, 011021. [CrossRef]

42. Cherstvy, A.G.; Thapa, S.; Wagner, C.E.; Metzler, R. Non-Gaussian, non-ergodic, and non-Fickian diffusion of tracers in mucin hydrogels. *Soft Matter* **2019**, *15*, 2526–2551. [CrossRef]
43. Lawley, S.D.; Miles, C.E. Diffusive search for diffusing targets with fluctuating diffusivity and gating. *J. Nonlinear Sci.* **2019**, *29*, 2955–2985. [CrossRef]
44. Sposini, V.; Chechkin, A.V.; Seno, F.; Pagnini, G.; Metzler, R. Random diffusivity from stochastic equations: Comparison of two models for Brownian yet non-Gaussian diffusion. *New J. Phys.* **2018**, *20*, 043044. [CrossRef]
45. Vitali, S.; Budimir, I.; Runfola, C.; Castellani, G. The role of the central limit theorem in the heterogeneous ensemble of Brownian particles approach. *Mathematics* **2019**, *7*, 1145. [CrossRef]
46. Postnikov, E.B.; Chechkin, A.; Sokolov, I.M. Brownian yet non-Gaussian diffusion in heterogeneous media: From superstatistics to homogenization. *New J. Phys.* **2020**, *22*, 063046. [CrossRef]
47. Lampo, T.J.; Stylianidou, S.; Backlund, M.P.; Wiggins, P.A.; Spakowitz, A.J. Cytoplasmic RNA-protein particles exhibit non-Gaussian subdiffusive behavior. *Biophys. J.* **2017**, *112*, 532–542. [CrossRef]
48. Stuhrmann, B.; e Silva, M.S.; Depken, M.; MacKintosh, F.C.; Koenderink, G.H. Nonequilibrium fluctuations of a remodeling in vitro cytoskeleton. *Phys. Rev. E* **2012**, *86*, 020901. [CrossRef]
49. Sabri, A.; Xu, X.; Krapf, D.; Weiss, M. Elucidating the origin of heterogeneous anomalous diffusion in the cytoplasm of mammalian cells. *Phys. Rev. Lett.* **2020**, *125*, 058101. [CrossRef] [PubMed]
50. Hidalgo-Soria, M.; Barkai, E. Hitchhiker model for Laplace diffusion processes. *Phys. Rev. E* **2020**, *102*, 012109. [CrossRef]
51. Rajesh, R.; Das, D.; Chakraborty, B.; Barma, M. Aggregate formation in a system of coagulating and fragmenting particles with mass-dependent diffusion rates. *Phys. Rev. E* **2002**, *66*, 056104. [CrossRef] [PubMed]
52. Sliusarenko, O.Y.; Vitali, S.; Sposini, V.; Paradisi, P.; Chechkin, A.; Castellani, G.; Pagnini, G. Finite-energy Lévy-type motion through heterogeneous ensemble of Brownian particles. *J. Phys. Math. Theor.* **2019**, *52*, 095601. [CrossRef]
53. Beck, C. Superstatistical Brownian motion. *Prog. Theor. Phys. Suppl.* **2006**, *162*, 29–36. [CrossRef]
54. Hapca, S.; Crawford, J.W.; Young, I.M. Anomalous diffusion of heterogeneous populations characterized by normal diffusion at the individual level. *J. R. Soc. Interface* **2009**, *6*, 111–122. [CrossRef] [PubMed]
55. Jeon, J.H.; Javanainen, M.; Martinez-Seara, H.; Metzler, R.; Vattulainen, I. Protein crowding in lipid bilayers gives rise to non-Gaussian anomalous lateral diffusion of phospholipids and proteins. *Phys. Rev. X* **2016**, *6*, 021006. [CrossRef]
56. dos Santos, M. A. F. Mittag-Leffler functions in superstatistics. *Chaos Solitons Fractals* **2020**, *131*, 109484. [CrossRef]
57. Sánchez, E. Burr type-XII as a superstatistical stationary distribution. *Physica A* **2019**, *516*, 443–446. [CrossRef]
58. Mathai, A.; Haubold, H.J. Mittag-Leffler functions to pathway model to Tsallis statistics. *Integral Transform. Spec. Funct.* **2010**, *21*, 867–875. [CrossRef]
59. Agahi, H.; Khalili, M. Truncated Mittag-Leffler distribution and superstatistics. *Physica A* **2020**, 555, 124620. [CrossRef]
60. Mura, A.; Taqqu, M.S.; Mainardi, F. Non-Markovian diffusion equations and processes: Analysis and simulations. *Physica A* **2008**, *387*, 5033–5064. [CrossRef]
61. Mura, A.; Mainardi, F. A class of self-similar stochastic processes with stationary increments to model anomalous diffusion in physics. *Integral Transform. Spec. Funct.* **2009**, *20*, 185–198. [CrossRef]
62. Pagnini, G. Erdélyi-Kober fractional diffusion. *Fract. Calc. Appl. Anal.* **2012**, *15*, 117–127. [CrossRef]
63. Molina-García, D.; Pham, T.M.; Paradisi, P.; Manzo, C.; Pagnini, G. Fractional kinetics emerging from ergodicity breaking in random media. *Phys. Rev. E* **2016**, *94*, 052147. [CrossRef]
64. Pagnini, G.; Paradisi, P. A stochastic solution with Gaussian stationary increments of the symmetric space-time fractional diffusion equation. *Fract. Calc. Appl. Anal.* **2016**, *19*, 408–440. [CrossRef]
65. Rojas-Nandayapa, L. Risk Probabilities: Asymptotics and Simulation. Ph.D. Thesis, Aarhus Universitetsforlag, Aarhus, Denmark, 2008.
66. Asmussen, S.; Jensen, J.L.; Rojas-Nandayapa, L. On the Laplace transform of the lognormal distribution. *Methodol. Comput. Appl. Probab.* **2016**, *18*, 441–458. [CrossRef]
67. Holgate, P. The lognormal characteristic function. *Commun. Stat. Theory Methods* **1989**, *18*, 4539–4548. [CrossRef]

68. Touchette, H.; Beck, C. Asymptotics of superstatistics. *Phys. Rev. E* **2005**, *71*, 016131. [CrossRef] [PubMed]
69. Rabassa, P.; Beck, C. Extreme value laws for superstatistics. *Entropy* **2014**, *16*, 5523–5536. [CrossRef]
70. Butler, R.W. *Saddlepoint Approximations with Applications*; Cambridge University Press: Cambridge, MA, USA, 2007; Volume 22.
71. Lim, S.; Muniandy, S. Self-similar Gaussian processes for modeling anomalous diffusion. *Phys. Rev. E* **2002**, *66*, 021114. [CrossRef]
72. Bodrova, A.S.; Chechkin, A.V.; Sokolov, I.M. Scaled Brownian motion with renewal resetting. *Phys. Rev. E* **2019**, *100*, 012120. [CrossRef]
73. Bodrova, A.S.; Chechkin, A.V.; Cherstvy, A.G.; Metzler, R. Ultraslow scaled Brownian motion. *New J. Phys.* **2015**, *17*, 063038. [CrossRef]
74. Fuliński, A. Anomalous diffusion and weak nonergodicity. *Phys. Rev. E* **2011**, *83*, 061140. [CrossRef]
75. Safdari, H.; Cherstvy, A.G.; Chechkin, A.V.; Thiel, F.; Sokolov, I.M.; Metzler, R. Quantifying the non-ergodicity of scaled Brownian motion. *J. Phys. Math. Theor.* **2015**, *48*, 375002. [CrossRef]
76. Sposini, V.; Metzler, R.; Oshanin, G. Single-trajectory spectral analysis of scaled Brownian motion. *New J. Phys.* **2019**, *21*, 073043. [CrossRef]
77. Mainardi, F.; Pagnini, G.; Gorenflo, R. Mellin transform and subordination laws in fractional diffusion processes. *Fract. Calc. Appl. Anal.* **2007**, *6*, 441.
78. Saxton, M.J. Anomalous subdiffusion in fluorescence photobleaching recovery: A Monte Carlo study. *Biophys. J.* **2001**, *81*, 2226–2240. [CrossRef]
79. Fieremans, E.; Burcaw, L.M.; Lee, H.H.; Lemberskiy, G.; Veraart, J.; Novikov, D.S. In vivo observation and biophysical interpretation of time-dependent diffusion in human white matter. *NeuroImage* **2016**, *129*, 414–427. [CrossRef]
80. Molini, A.; Talkner, P.; Katul, G.G.; Porporato, A. First passage time statistics of Brownian motion with purely time dependent drift and diffusion. *Physica A* **2011**, *390*, 1841–1852. [CrossRef]
81. Metzler, R. Brownian motion and beyond: First-passage, power spectrum, non-Gaussianity, and anomalous diffusion. *J. Stat. Mech. Theory Exp.* **2019**, *2019*, 114003. [CrossRef]
82. Chubynsky, M.V.; Slater, G.W. Diffusing diffusivity: A model for anomalous, yet Brownian, diffusion. *Phys. Rev. Lett.* **2014**, *113*, 098302. [CrossRef] [PubMed]
83. Wang, W.; Cherstvy, A.G.; Chechkin, A.V.; Thapa, S.; Seno, F.; Liu, X.; Metzler, R. Fractional Brownian motion with random diffusivity: Emerging residual nonergodicity below the correlation time. *J. Phys. Math. Theor.* **2020**. [CrossRef]
84. Wang, W.; Seno, F.; Sokolov, I.M.; Chechkin, A.V.; Metzler, R. Unexpected crossovers in correlated random-diffusivity processes. *New J. Phys.* **2020**, *22*, 083041. [CrossRef]